

## Introduction

Manifold learning techniques have become of great interest when studying high dimensional data.

- Usually, the data have an extrinsic dimensionality that is artificially high, while its intrinsic structure is well-modeled as a low-dimensional manifold plus noise.
- Following the same line of reasoning, dynamical systems and time series can be regarded as processes governed by few underlying parameters, confined in a low-dimensional manifold.

**Goal:** Discover low-dimensional representations of high dimensional dynamical systems.

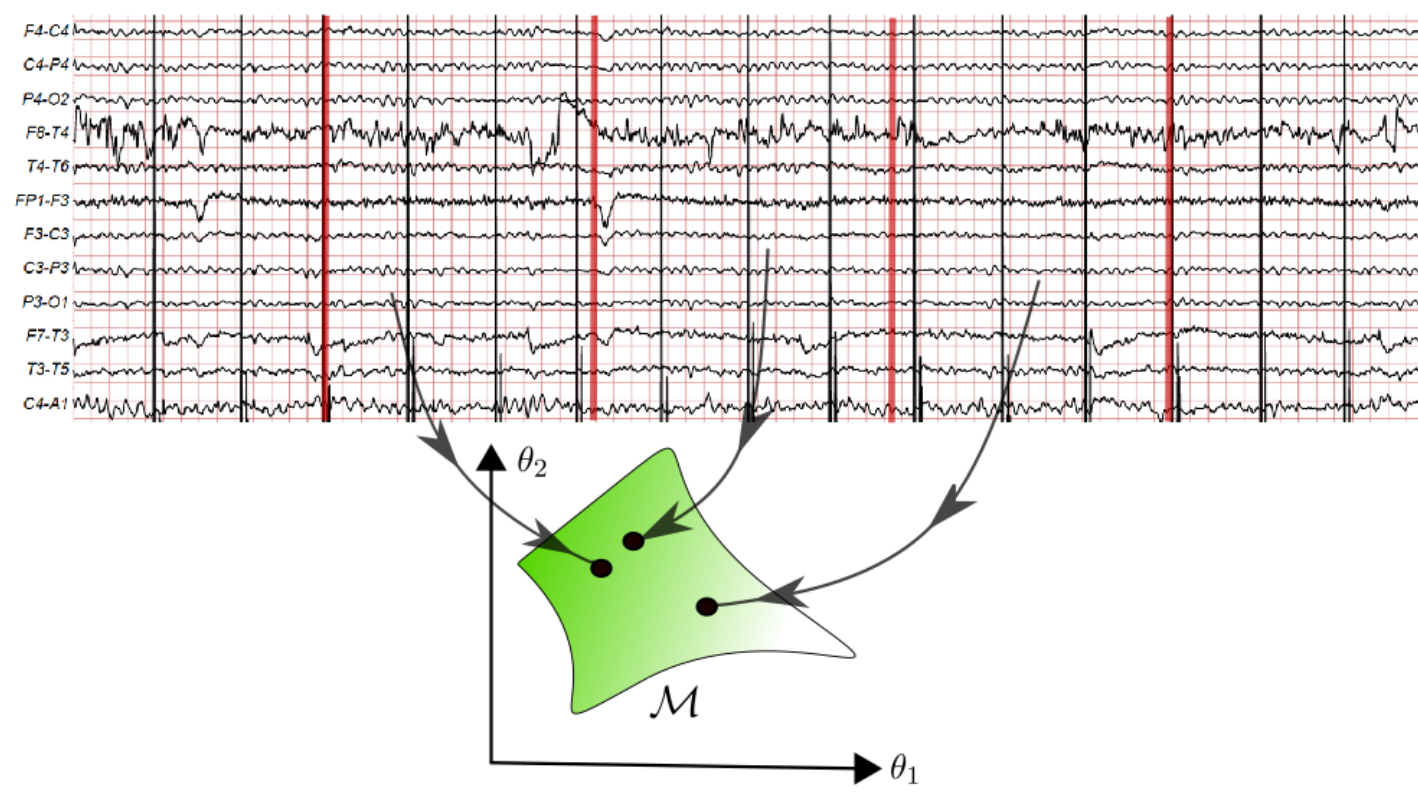


Figure 1: The process can be visualized in a low dimensional representation in the space of some underlying parameters  $\theta$  driving the system. The figure shows a 12-dimensional dynamical system. And the goal is to represent time windows of the data as points in a low-dimensional manifold.

## Contributions:

- A novel manifold learning technique for dynamical systems called **DIG** (Dynamical information geometry).
- Incorporation of a novel group of distances in the context of diffusion operators.

## Manifold Learning with Diffusion Operators

The use of diffusion operators in manifold learning was first introduced in Diffusion Maps [1]. Recently, more suited algorithms for visualization have been presented, such as PHATE [3]:

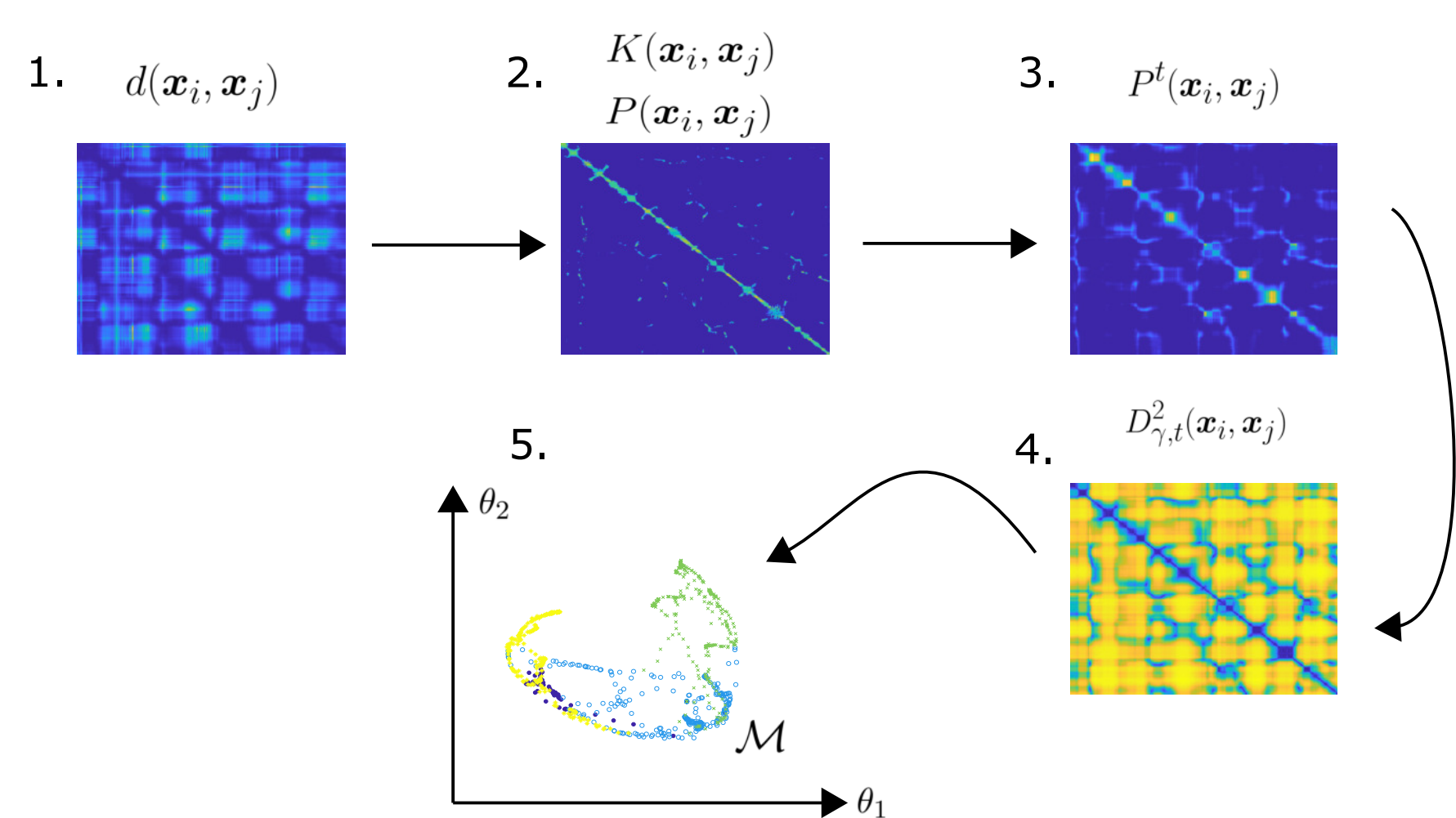


Figure 2: **PHATE steps.** 1. Compute the distances between observations, typically the euclidean distance is employed in this step. 2. Apply an adaptive kernel function to  $d(x_i, x_j)$ , and then row-normalize it to create a row stochastic matrix called the potential operator. 3. Diffuse the potential operator  $t$ -steps forward. 4. Compute an information distance between the rows of  $P^t$ . Finally in 5, apply metric MDS to  $D_{\gamma,t}^2$ .

- Diffusion Maps encapsulates the information in many dimensions.
- PHATE captures information in fewer dimensions  $\Rightarrow$  better for visualization.

## Diffusion with Dynamical Systems

In the context of dynamical systems we learn the local structure by constructing a matrix that encodes the local distances between time windows of data.

### State-space formalism:

$$\mathbf{x}_t = \mathbf{y}_t(\boldsymbol{\theta}_t) + \boldsymbol{\xi}_t \quad (1)$$

$$d\boldsymbol{\theta}_t^i = a^i(\boldsymbol{\theta}_t^i)dt + dw_t^i, \quad i = 1, \dots, d. \quad (2)$$

- $p(\mathbf{x}|\boldsymbol{\theta})$  is a linear transformation of  $p(\mathbf{y}|\boldsymbol{\theta})$
- New feature space, obtained by the histogram bins of the data within time windows of length  $L_1$  centered at  $\mathbf{x}_t$ :

$$\mathbf{x}_t \Rightarrow \mathbf{h}_t$$

- The expected value of the histograms, e.g.  $\mathbb{E}(\mathbf{h}_t^i)$ , is a linear transformation of  $p(\mathbf{x}|\boldsymbol{\theta})$
- The Mahalanobis distance is invariant under linear transformations.
- $\Rightarrow$  Distance (3) is noise resilient [4, 5]

$$d^2(\mathbf{x}_t, \mathbf{x}_s) = (\mathbb{E}(\mathbf{h}_t) - \mathbb{E}(\mathbf{h}_s))^T (\mathbf{C}_t)^{-1} (\mathbb{E}(\mathbf{h}_t) - \mathbb{E}(\mathbf{h}_s)), \quad (3)$$

### Alternative distance:

Assumes that the data within time windows of length  $L_1$  centered at  $x_t$  follows a multivariate Gaussian distribution  $\mathcal{N}(\boldsymbol{\mu}, \Sigma_t)$ .

- The geodesic distance between different time windows of data centered at  $\mathbf{x}_t$  and  $\mathbf{x}_s$  using the Fisher information as the Riemannian metric is as follows:

$$d^2(\mathbf{x}_t, \mathbf{x}_s) = \frac{1}{2} \sum_{i=1}^N \ln(\lambda_i), \quad \text{where } |\Sigma_t - \lambda_i \Sigma_s| = 0 \quad (4)$$

## Information Distances

DIG extracts the information from the diffusion operator by embedding an information distance. We focus on a broad family of information distances that are parametrized by  $\gamma$ :

$$D_{\gamma,t}^2(\mathbf{x}_i, \mathbf{x}_j) = \begin{cases} \sum_{k=1}^N \frac{(\log P_{ki}^t - \log P_{kj}^t)^2}{\phi_0(k)}, & \gamma = 1 \\ \sum_{k=1}^N \frac{(P_{ki}^t - P_{kj}^t)^2}{\phi_0(k)}, & \gamma = -1 \\ \sum_{k=1}^N \frac{2((P_{ki}^t)^{\frac{1-\gamma}{2}} - (P_{kj}^t)^{\frac{1-\gamma}{2}})^2}{(1-\gamma)\phi_0(k)}, & -1 < \gamma < 1. \end{cases} \quad (5)$$

Additionally, the rows of the diffusion matrix  $P$  can be interpreted as multinomial distributions. The geodesic distance between them using the Fisher information as the Riemannian metric is as follows:

$$D(\mathbf{x}_i, \mathbf{x}_j) = 2\cos^{-1} \left( \sum_{k=1}^N \sqrt{P_{ki}^t P_{kj}^t} \right). \quad (6)$$

After the information distances have been obtained, DIG applies metric multidimensional scaling (MDS) to the information distances to obtain a low-dimensional representation

## Algorithm

### Algorithm 1 The DIG algorithm

**Input:** Data matrix  $X$ , neighborhood size  $k$ , locality scale  $\alpha$ , time windows length  $L_1$  and  $L_2$ , number of bins  $Nb$ , information parameter  $\gamma$ , desired embedding dimension  $m$  (usually 2 or 3 for visualization)

**Output:** The DIG embedding  $Y_m$

- 1:  $d \leftarrow$  compute pairwise distance matrix from  $X$  using the mahalanobis distance (3)
- 2:  $K_{k,\alpha} \leftarrow$  compute local affinity matrix from  $d$  and  $\sigma_k$
- 3:  $P \leftarrow$  normalize  $K_{k,\alpha}$  to form a Markov transition matrix (diffusion operator)
- 4:  $t \leftarrow$  compute time scale via Von Neumann Entropy [3]
- 5: Diffuse  $P$  for  $t$  time steps to obtain  $P^t$
- 6:  $D_{\gamma,t}^2 \leftarrow$  compute the information distance matrix in eq. 5 from  $P^t$  for the given  $\gamma$
- 7:  $Y^t \leftarrow$  apply classical MDS to  $D_{\gamma,t}^2$
- 8:  $Y_m \leftarrow$  apply metric MDS to  $D_{\gamma,t}^2$  with  $Y^t$  as an initialization

## Results in real data

We applied DIG to EEG data provided by [6, 2]. The data is labeled with one of six sleep categories according to R&K rules (REM, Awake, S-1, S-2, S-3, S-4). Due to the lack of observations in some stages, we group S-1 with S-2, and S-3 with S-4. We band-filtered the data between 8-40 Hz, and down-sampled it to 128Hz.

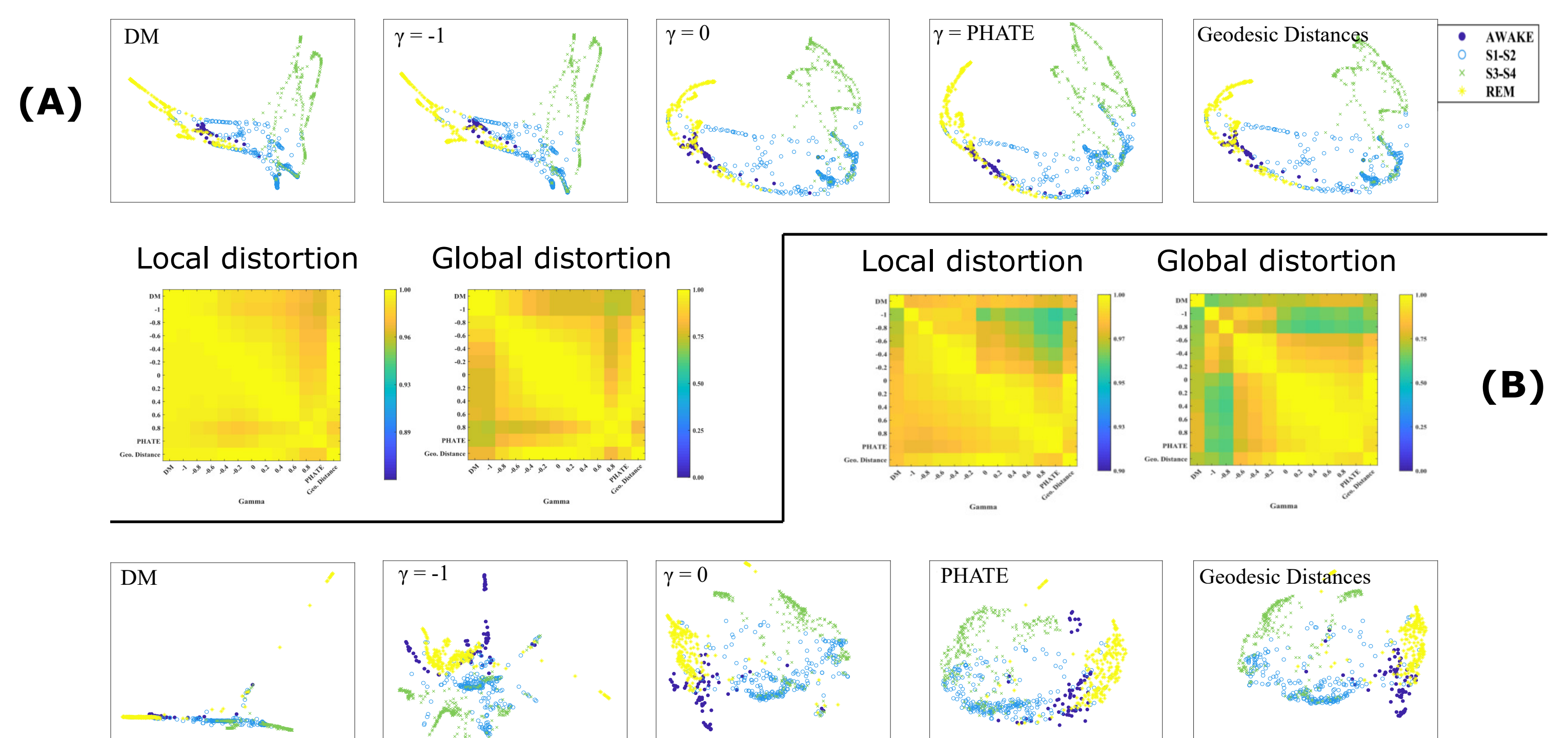


Figure 3: **(A)** Shows the embeddings obtained by the mahalanobis distance (3), for different values of  $\gamma$ . Additionally, we compare the relative local and global distortion of the embeddings, measured by the Trustworthiness and the Mantel test respectively. The same is replicated in **(B)** but for the gaussian information distance (4).

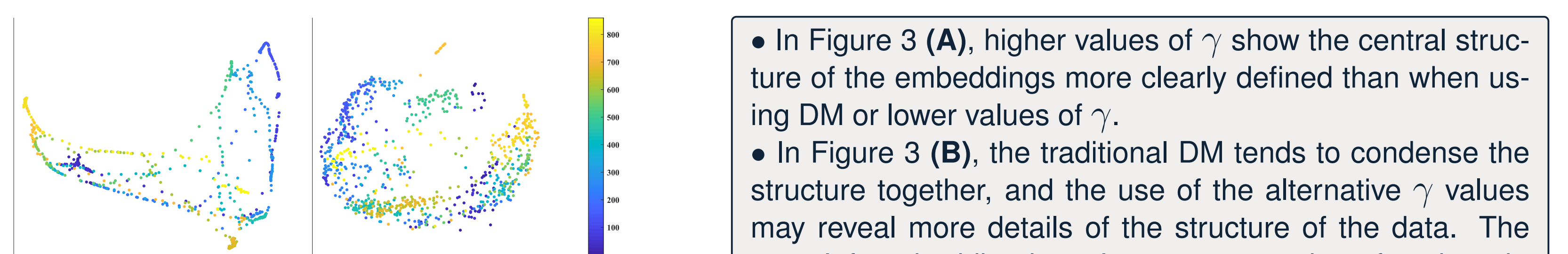


Figure 4: Visualization of EEG data colored by time steps using distance (3) at the left, and distance (4) at the right. Here we see how the left visualization presents a more denoised version, with clearer time-evolving transitions.

- In Figure 3 **(A)**, higher values of  $\gamma$  show the central structure of the embeddings more clearly defined than when using DM or lower values of  $\gamma$ .
- In Figure 3 **(B)**, the traditional DM tends to condense the structure together, and the use of the alternative  $\gamma$  values may reveal more details of the structure of the data. The most left embedding is a clear representation of such a situation, where DM does not show a suitable discrimination of the sleep stages. But when the value of gamma is increased, a more suitable representation is achieved.

## Conclusions

- We derived a manifold learning tool called DIG for visualizing dynamical processes based on a diffusion framework. We addressed some of the shortcomings of the traditional diffusion maps approach for visualization.
- We presented experimental results where we were able to discover sleep dynamics using solely EEG recordings, as well as the time-varying progress of the processes.
- We presented a new group of distances in the context of diffusion operators.

## References

- [1] R.R. Coifman and S. Lafon. "Diffusion maps". In: *Applied and computational harmonic analysis* 21.1 (2006), pp. 5–30.
- [2] A.L. Goldberger et al. "PhysioBank, PhysioToolkit, and PhysioNet: components of a new research resource for complex physiologic signals". In: *Circulation* 101.23 (2000), e215–e220.
- [3] K.R. Moon et al. "Visualizing transitions and structure for biological data exploration". In: *Nature Biotechnology (to appear)* (2019).
- [4] R. Talmon and R.R. Coifman. "Empirical intrinsic geometry for nonlinear modeling and time series filtering". In: *Proceedings of the National Academy of Sciences* 110.31 (2013), pp. 12535–12540.
- [5] R. Talmon and R.R. Coifman. "Intrinsic modeling of stochastic dynamical systems using empirical geometry". In: *Applied and Computational Harmonic Analysis* 39.1 (2015), pp. 138–160.
- [6] M.G. Terzano et al. "Atlas, rules, and recording techniques for the scoring of cyclic alternating pattern (CAP) in human sleep". In: *Sleep medicine* 3.2 (2002), pp. 187–199.